PET Imaging of Leptin Biodistribution and Metabolism in Rodents and Primates

Giovanni Ceccarini[1,*], **Robert R Flavell**[2,*], **Eduardo R Butelman**[4], **Michael Synan**[3], **Thomas E Willnow**[5], **Maya Bar-Dagan**[2], **Stanley J Goldsmith**[3], **Mary J Kreek**[4], **Paresh Kothari**[3], **Shankar Vallabhajosula**[3], **Tom W Muir**[2,ˆ], and **Jeffrey M Friedman**[1,]

[1]Laboratory of Molecular Genetics, Howard Hughes Medical Institute, The Rockefeller University, New York, NY 10065

[2]Laboratory of Synthetic Protein Chemistry, The Rockefeller University

[3]Citigroup Biomedical Imaging Center Weill Cornell Medical College, Cornell University, New York, NY 10065

[4]Laboratory on the Biology of Addictive Diseases, The Rockefeller University

[5]Max-Delbrueck Center for Molecular Medicine, Berlin

Summary

Here we report the first PET imaging studies of leptin's systemic biodistribution in vivo. PET imaging using ^{18}F and ^{68}Ga labeled leptin revealed that in mouse the hormone was rapidly taken up by megalin (gp330/LRP2), a multiligand endocytic receptor localized in renal tubules. In addition, in rhesus monkeys 15% of labeled leptin localized to red bone marrow which was consistent with hormone uptake in rodent tissues. These data confirm a megalin-dependent mechanism for renal uptake in vivo. The significant binding to immune cells and blood cell precursors in bone marrow is also consistent with prior evidence showing that leptin modulates immune function. These experiments set the stage for similar studies in humans to assess the extent to which alterations of leptin's biodistribution might contribute to obesity and also provide a novel and general chemical strategy for ^{18}F labeling of proteins for PET imaging of other polypeptide hormones.

Introduction

Leptin is a 16 kDa protein hormone secreted by adipocytes, which regulates body weight by reducing food intake and increasing energy expenditure (Coll et al., 2007; Friedman and Halaas, 1998). Leptin also signals nutritional status to several other physiological systems and modulates their function. The leptin receptor is a cytokine family receptor with several isoforms that are generated by alternative splicing. Genetic evidence has indicated that leptin's biologic effects are principally the result of binding to the Lep-Rb isoform, which is the only splice variant of the leptin receptor that expresses all of the motifs required for signal transduction. Genetic evidence has further suggested that this isoform is necessary for leptin to exert its weight suppressing effects. Lep-Rb is expressed primarily in brain and on hematopoietic and

ˆCorrespondence should be addressed to TWM (muirt@mail.rockefeller.edu) and JMF (friedj@mail.rockefeller.edu).
*Authors with equal contribution

immune cells, while the other splice variants show a broad tissue distribution including kidney, liver, lung and spleen (Fei et al., 1997). While leptin signaling in the central nervous system is both necessary (Cohen et al., 2001) and sufficient (de Luca et al., 2005) to generate leptin's metabolic effects, direct actions on peripheral tissues have also been described (Lord et al., 1998; Morioka et al., 2007; Sierra-Honigmann et al., 1998).

In this study we set out to further assess the biodistribution and metabolism of leptin using Positron Emission Tomography imaging. PET is well suited for studies of the biodistribution of hormones due to its mm scale resolution, high sensitivity, and ease of quantification (Bailey et al., 2005). While a previous report used PET imaging to study the CNS distribution of leptin following intrathecal injection (McCarthy et al., 2002), PET imaging has not been used to comprehensively study leptin's systemic biodistribution. Here we describe the development of two positron labeled leptin tracers, ^{18}F-FBA-leptin and ^{68}Ga-DOTA-leptin. The use of PET in mutant mice has confirmed that leptin metabolism by renal cortex is mediated by megalin and not Lep-R despite the high levels of Lep-R gene expression in this tissue. We also show a high level of leptin uptake in hematopoietic tissues in rodents and monkeys, consistent with a role for leptin in modulating the physiology of hematopoiesis and/or immune function.

Results

Development of leptin tracers

Two leptin tracers were generated: ^{18}F-FBA-leptin and ^{68}Ga-DOTA-leptin which label the C-terminus or amino groups respectively. Mutagenesis studies have identified residues of leptin which are required for receptor binding and activation (Peelman et al., 2004; Verploegen et al., 1997) and overall these studies indicate that lysine residues of the protein as well as the C and N termini of the molecule are not critical for receptor binding and activation (Zhang et al., 1997). We thus reasoned that either an amine-directed or a site-specific C-terminal labeling strategy would produce a labeled leptin derivative with unaltered bioactivity and moreover that consistent results for both tracers would confirm the bona fide distribution of the hormone (Fig. 1a). ^{68}Ga-DOTA-leptin was labeled using conventional methods. In order to label leptin with ^{18}F we employed a recently developed strategy that can specifically label the C-terminus of proteins in a site specific manner, using expressed protein ligation followed by an oximation reaction (Supplemental Fig. 1) (Flavell et al., 2008). This tracer, named ^{18}F-FBA-Leptin, retains biological activity and, because ^{18}F is a lower energy positron emitter, allows for high-resolution micro-PET imaging (Flavell et al., 2008).

Leptin was labeled with ^{68}Ga using the chelator DOTA (Fig. 1b). An average of 4 DOTA moieties were incorporated per leptin molecule using DOTA-NHS (De Leon-Rodriguez and Kovacs, 2008) (Fig. 1c). The modified protein retained its ability to activate STAT3-dependent Lep-R signaling in a cell line stably transfected with leptin receptor (Fig. 1d), and was also able induce weight loss in leptin deficient (ob/ob) mice with similar potency to unmodified recombinant leptin (Fig. 1e). The decay-corrected radiochemical yield of ^{68}Ga-DOTA-leptin was 25.7% ± 4.9% s.d., (n = 30, specific activity of 5.5 – 11 GBq/μmol, Supplemental Fig. 2), with a product that was greater than 90% pure (Fig. 1f). The tracer was stable *in vivo* as assessed by radiochemical HPLC analysis of the serum recovered from a mouse injected 30 min prior (Fig. 1f). Finally, the ^{68}Ga labeling procedure did not abrogate receptor binding activity, as the labeled protein bound to the cell line expressing Lep-R, and this binding could be displaced by excess competing cold leptin (Fig. 1g). As mentioned above, ^{18}F-FBA-Leptin was labeled and the tracer was validated in vitro and in vivo as described (Flavell et al., 2008). Overall, we have developed two positron emitting leptin tracers using complementary labeling chemistries and isotopes, one of which is site specific, and both tracers retained bioactivity in vivo and in vitro.

Whole body PET scans

We analyzed the biodistribution of leptin in mice and rats using both ^{68}Ga-DOTA and ^{18}F-FBA tracers. PET imaging of both tracers after injection into ob/ob mice revealed that leptin accumulates principally in the kidneys, and to a much lesser extent in several other visceral organs including liver and spleen, as well as the head (Fig. 2a, b). Uptake of the tracers was not observed in fat and brain. The superior resolution of ^{18}F compared to ^{68}Ga further allowed us to visualize the accumulation of the tracer in the renal cortex in mice (Fig. 2b, d). This finding was also confirmed using ^{68}Ga-DOTA-leptin in rats (Fig. 2c). These data indicated that leptin is filtered by the kidney and taken up by renal tubular cells where it is likely to be metabolized, a possibility consistent with previous reports (Cumin et al., 1996; Klein et al., 1996; Meyer et al., 1997; Zeng et al., 1997).

Quantitative analysis of kidney uptake

Kinetic analysis of uptake with our tracers in the kidney revealed that ^{68}Ga radioactivity remained in the kidney for an extended period after ^{68}Ga-DOTA-leptin injection (i.e., the tracer and/or its metabolites are trapped intra-cellularly), while ^{18}F-FBA-leptin did not, consistent with previous reports using tracers labeled with similar methods (Supplementary Fig. 3) (Schottelius et al., 2004; Tsai et al., 2001). Thus, ^{68}Ga-DOTA-leptin was used in a series of quantitative kinetic studies.

Thirty minutes after injection of the tracer, $68.2 \pm 1.5\%$ was localized to the kidney (Fig. 3c). Radiochemical HPLC analysis of kidney extracts from mice injected with the tracer showed a peak eluting at 3 min, in contrast to intact leptin, which elutes at 21.6 minutes, indicating that the leptin was degraded in this organ (Fig. 3a). When the tracer was co-injected with a 30 fold excess of cold ligand, $23.7 \pm 2.2\%$ of the leptin was displaced from the kidney and instead appeared in the bladder (Fig. 3c). Radiochemical HPLC analysis of the urine of these animals revealed a peak eluting at 21.6 min, indicating that intact leptin is displaced from the kidney receptors (Fig. 3b). These results suggested that leptin uptake by the renal tubular cells is mediated by a saturable receptor mediated mechanism and that leptin is degraded after being taken up by these cells.

Kidney uptake of leptin in ob/ob and ob/ob-Lep-RΔ mice

Lep-R is expressed in the kidney, raising the possibility that it might be responsible for the renal uptake of leptin (Fei et al., 1997; Hama et al., 2004). In order to test this hypothesis we compared the renal uptake of the tracer in wild type mice, leptin deficient (ob/ob) and mice with a null mutation of the leptin receptor. In order to address the possible confounding effect of secondarily elevated high endogenous leptin levels in Lep-R deficient mice (which have a null Lep-R mutation), Lep-RΔ mutant mice were mated to ob mice and the studies were performed in mice that carried mutations in both leptin and its receptor (referred to as ob/ob-Lep-RΔ mice) (Cohen et al., 2001). This allows a direct comparison of the biodistribtion of the leptin tracer in ob/ob mice +/- the leptin receptor. Time activity curves of kidney uptake in these three experimental groups are identical (Fig. 3d). These data suggested that the renal uptake of leptin was not mediated by the leptin receptor, and rather a different receptor was responsible.

Renal uptake and metabolism of leptin in megalin kidney knockout mice

We next considered the possibility that leptin uptake by the kidney was mediated by megalin (gp330/LRP2). Megalin is a high molecular weight multiligand receptor that is expressed in the proximal convoluted tubule in the kidney and other tissues (Christensen and Birn, 2002). Previous studies have shown that megalin mediates the renal uptake of several hormones. In addition, previous studies have also shown that leptin is capable of binding to megalin in vitro

with an affinity of 200 nM (Hama et al., 2004). In order to test the role of megalin in renal uptake of leptin, we studied mice with a kidney specific megalin knockout (termed megalin[lox/lox], ApoE[cre]) (Leheste et al., 2003). The renal expression of the receptor is reduced to ~ 10% of normal levels in the megalin[lox/lox], ApoE[cre] mice (Leheste et al., 2003).

Leptin is undetectable in the urine of wild type rodents so we began by measuring the urine levels of leptin in the knockout mice by ELISA. Leptin levels in the urine of megalin[lox/lox], ApoE[cre] mice levels were 16.7 ± 2.9 ng/mL (n=4 ± SEM) indicating a significant excretion of leptin in urine in the knockout mice (Fig. 4a). The urinary leptin was intact as confirmed by Western blotting (Fig. 4b).

These results suggest that leptin is filtered by the renal glomerulus and taken up in the proximal convoluted tubule in a megalin dependent manner. To confirm this, we performed PET imaging of megalin[lox/lox], ApoE[cre] mice using ^{68}Ga-DOTA-leptin. These studies showed that, similar to the effect of adding an excess of cold leptin, the level of the tracer in the bladder of megalin[lox/lox], ApoE[cre] mice is significantly increased and that the uptake by the kidney is significantly reduced when compared to littermate controls (Fig. 4c, d, f, g). Note, that there is some residual uptake of the tracer in the renal cortex of megalin[lox/lox], ApoE[cre] mice, attributable to the fact that the megalin knockout is incomplete in kidney (Supplemental Fig. 4). Radiochemical HPLC analysis of the urine from a megalin[lox/lox], ApoE[cre] mouse revealed the characteristic peak of intact leptin (Fig. 4e). In aggregate, these data show that leptin is freely filtered by the glomerulus and that megalin is required for the uptake and metabolism of the hormone in the proximal convoluted tubule.

Leptin uptake is mediated by megalin in vitro

Megalin also mediates the uptake of other hormones as well as aminoglycoside antibiotics. We studied the degradation of ^{125}I-leptin by megalin-expressing L2 cells, as previously described (Hama et al., 2004). Similar to other peptides, ^{125}I-leptin is degraded by these cells. In L2 cells, leptin degradation is inhibited in a dose dependent manner by cold leptin (Fig. 4h). Leptin degradation is also inhibited by the known megalin inhibitor, receptor associated protein, RAP (Supplemental Fig. 5, Fig. 4h) (Christensen and Birn, 2002). These data confirm that leptin is degraded after receptor mediated uptake by megalin *in vitro*.

Several peptides and proteins including parathyroid hormone (PTH), insulin, prolactin, and apolipoprotein J/clusterin, were also able to inhibit the degradation, while other ligands such as aminoglycoside did not (Fig. 4i, j). This result suggests that leptin likely binds to the same site of megalin as PTH, insulin, prolactin, and ApoJ. Overall these in vivo and in vitro data confirm that leptin metabolism is the result of binding to megalin followed by the intracellular degradation of the hormone.

Biodistribution analysis in mice

The absence of a leptin signal in other tissues after PET imaging does not exclude the possibility that leptin binds there as the sensitivity of PET imaging is limited by the total number of binding sites and the specific activity of the tracer. In order to further assess the extent to which leptin could bind to Lep-R in other tissues we performed biodistribution analysis using ^{125}I-leptin. In this experiment, a small amount (less than 100 ng vs. 20-30 μg in a PET experiment, supplemental table 2) of ^{125}I-leptin was injected +/- an excess of cold leptin, and animals were sacrificed 15 minutes later after which the radioactivity was quantitated in tissues.

We compared four groups of mice: wild type, ob/ob, Lep-RΔ, and the aforementioned ob/ob-Lep-RΔ (Supplemental Table 1). As above the ob/ob-Lep-RΔ were used so that we could robustly analyze leptin uptake without the confounding effect of hyperleptinemia which could

competitively inhibit leptin binding. Wild type mice showed saturable uptake of ^{125}I-leptin in the spleen, lung, liver, and intact femur (Fig. 5a). This was confirmed in studies of ob/ob mice, ob/ob mice with competing cold leptin injection, and ob/ob-Lep-RΔ mice, where we found saturable, Lep-R dependent uptake of leptin in the spleen, lung, liver, femur, fat, and brain (Fig. 5b-d). Collectively, these data suggest that Lep-R is required for leptin binding at high levels in the spleen, liver, lung, and femur, and also at low levels in the fat and brain. The binding of leptin in spleen and femur is consistent with the previous reports of direct effects of leptin on immune and hematopoietic cells (Bennett et al., 1996; Cioffi et al., 1996; Farooqi et al., 2002; Gainsford et al., 1996; Umemoto et al., 1997). This possibility was further assessed in studies of non-human primates, see below.

PET-CT of leptin biodistribution in rhesus macaques

We next performed PET-CT imaging in rhesus macaques. In addition to providing a potential basis for initiating PET imaging in humans, the use of monkeys for PET imaging often provides greater sensitivity owing to their larger size and the corresponding increase in the number of binding sites. PET imaging using both ^{68}Ga-DOTA-leptin and ^{18}F-FBA-leptin revealed that the tracer was again restricted to the cortex of the kidney, consistent with a megalin-dependent uptake mechanism (Fig. 6d). In addition to the kidney, there was highly significant leptin binding in sphenoid bone, mandible, vertebral bodies, sacrum, sternum, and the head of the humeri and femurs. Binding of leptin to these sites and not adjacent structures is clearly evident in the three dimensional reconstruction offered by the video file (Fig. 6a-b, e-h, Supplementary Video 1, 2). This pattern of uptake mimics the known pattern of red bone marrow in adult primates (Blebea et al., 2007). Pre-treatment of the monkey with 1 mg of unlabeled rhesus leptin or murine leptin, but not equimolar amounts of albumin (3.3 mg) as a negative control (Supplementary Fig. 6), 5 minutes prior to scanning blocked this signal, indicating that leptin binding at these sites is saturable and likely to be Lep-R mediated (Fig. 6c, Supplemental Fig. 7,8, Supplemental Videos 3, 4). At early time points (10-25 minutes post injection) a significant fraction of leptin can be seen in the blood pool fraction, including high levels in the chambers of the heart and great vessels. At later time points, nearly all of the leptin has localized in the bone marrow and kidney, or in kidney alone when competing leptin is present (Supplemental Fig. 9 and Videos 3-6). ^{18}F-FBA-leptin initially follows a similar bio-distribution to ^{68}Ga-DOTA-leptin, but as a consequence of tissue uptake and degradation (see above), its metabolites drain into the bladder (Supplemental Fig. 9).

Quantification of the uptake revealed that 15.8 and 16.4% of ^{68}Ga-DOTA-leptin and 14.1% of ^{18}F-FBA-leptin localized to and was retained in the bone marrow in a saturable manner, while there was no saturable uptake in the heart (Fig. 6i, j). These data show that in addition to kidney there is substantial leptin binding to red bone marrow in rhesus macaques, an observation that is consistent with leptin's known effects on immune function.

Discussion

Here we report the development, using complementary labeling chemistries and isotopes, of two fully bioactive tracers for studying leptin biodistribution, and their application to PET imaging in rodents and nonhuman primates. The methods described are widely applicable to study the in-vivo biodistribution of peptides and proteins hormones. The use of two tracers validates the results and also provides complementary information, with ^{18}F-FBA-Leptin allowing for high-resolution micro-PET imaging (Fig. 2b), and ^{68}Ga-DOTA-leptin providing a platform for a quantitative and kinetic analysis of leptin uptake (Fig. 3a, 3c, 4f, 4g, Supplemental Fig. 3).

Whole body PET images using our tracers revealed a similar bio-distribution in mice and rats with highly significant uptake in the renal cortex (Fig. 2b-d). This micro-PET rodent study

thus provided an opportunity to directly quantify leptin metabolism in the kidney where there was a high level of uptake and a similar biodistribution pattern in mice, rats and rhesus macaques (Fig. 2, 6d). In both humans and rodents, leptin has a short half-life, and the kidneys have been suggested to be the major site of leptin metabolism, accounting for over 80% of all clearance from plasma (Cumin et al., 1996; Klein et al., 1996; Meyer et al., 1997; Vila et al., 1998; Zeng et al., 1997). The finding of rapid and identical kidney uptake in several mouse strains, rats and monkeys, with approximately 50% of the total hormone appearing in the kidney 3 min post injection, is consistent with this evidence suggesting that leptin is metabolized by the kidney. The clearance of potent low molecular weight hormones such as leptin by the kidney may have clinical significance because end stage renal disease (ESRD) causes increased leptin levels (Merabet et al., 1997) and could thus contribute to the anorexia of ESRD.

Both the long (Lep-Rb) and one of the short (Lep-Ra) isoforms of leptin receptor are expressed in kidney mainly at the loop of Henle (Hama et al., 2004), and both forms are capable of mediating the internalization of leptin in vitro (Hileman et al., 2000). However, the observation that renal uptake of leptin is identical in mice with or without the leptin receptor suggested that its uptake was mediated by a different receptor. We thus tested whether this uptake was mediated by megalin.

Megalin is highly expressed in the proximal convoluted tubule of the renal cortex and mediates the endocytosis of several ligands, including hormones and their precursors (PTH, insulin, prolactin, EGF, thyroglobulin) vitamin binding proteins (Vit-D binding protein, retinol binding protein, transcobalamin) and other carrier proteins (haemoglobin, myoglobin, albumin, lactoferrin, transthyretin) (Christensen and Birn, 2002). Mice with a kidney specific knockout of megalin (megalin$^{lox/lox}$, ApoE^{cre}) show reduced renal uptake of several megalin ligands (de Jong et al., 2005; Leheste et al., 2003; Raila et al., 2005). Several lines of evidence confirm that megalin (gp330/LRP2), and not Lep-R, mediates leptin metabolism in the kidney *in vivo*. Firstly, leptin directly binds to megalin with an affinity of 200 nM (Hama et al., 2004). Furthermore, there are increased levels of intact leptin in the urine of megalin$^{lox/lox}$, ApoE^{cre} mice and the uptake of leptin in the kidneys in these animals is reduced in a PET imaging assay. Finally, we showed that leptin can be degraded by the megalin expressing L2 yolk sac tumor cell line, and also found that the degradation can be inhibited by other known megalin ligands (Fig. 4h, j). Thus, megalin, and not Lep-R, is responsible for the binding and uptake of leptin by the renal tubular cells after filtration of the protein by the glomerulus. Once leptin is taken up by the renal tubular cells, is degraded.

These results also raise the possibility that megalin could play a role in other aspects of leptin physiology. Megalin is expressed in lung, intestine, thyroid, parathyroid, placenta, endometrium, yolk sac, epididymis, ovary and, importantly, in brain microvessels and choroid plexus (Zlokovic et al., 1996). These latter two anatomical structures comprise the blood-CSF barrier (Christensen and Birn, 2002), suggesting that megalin, expressed at lower level (and mass) than the kidney, could play a role in the transport or metabolism of leptin in the brain, the mechanism for which has not been elucidated. It was recently shown that in rats, the delivery of lentiviral vectors containing siRNA directed against megalin reduced leptin levels in cerebrospinal fluid as assessed by Western blot (Dietrich et al., 2008). Our finding that leptin is cleared in a megalin dependent manner in the renal cortex is consistent with the possibility that megalin may play a role in the uptake or metabolism of leptin in additional sites, a possibility that can be tested in mice with megalin knockouts in other organs, now underway. In this case megalin could become an important drug target to improve leptin action.

The biodistribution and PET experiments of leptin reveal a high level of uptake in tissues undergoing active hematopoiesis, specifically the bone marrow in rhesus monkeys and the bone marrow and spleen in mice (Galloway and Zon, 2003). This includes the demonstration

that leptin binding in the bone marrow and spleen is Lep-R dependent in mice, and the fact that bone marrow binding of leptin in rhesus macaques can be saturated at only 0.1 mg/kg injected dose of leptin. These results are consistent with known Lep-R expression in hematopoietic precursors (Bennett et al., 1996; Cioffi et al., 1996) and the observation that leptin has direct effects on hematopoietic precursors and bone marrow stromal cells *in vitro* (Gainsford et al., 1996; Thomas et al., 1999; Umemoto et al., 1997). In addition, leptin deficient mice and humans are immunocompromised, in a manner that can be reversed with leptin treatment, revealing that leptin's role in regulating the immune system and hematopoiesis is required for normal immune and hematopoietic function (Claycombe et al., 2008; Farooqi et al., 2002; Lord et al., 1998; Palmer et al., 2006). While the similar data in all species tested suggest that leptin uptake in the bone marrow in rhesus monkeys is LepR dependent, further experiments are necessary to confirm this observation. A characterization of the cell types responsible for leptin uptake in the bone marrow could confirm the requirement for LepR for leptin binding and help to elucidate its role in hematopoiesis, immunity, and adipose tissue development.

We were unable to detect Lep-R dependant interactions in mice in our micro-PET experiments, including in the fat and at the hypothalamic binding sites that are required for leptin's role in regulating food intake and energy expenditure. Based on the finding that we could detect saturable binding of leptin in rhesus macaques in the bone marrow at an injected dose of 0.006 mg/kg but not 0.1 mg/kg, we predict that an injected dose of less than 0.005 mg/kg would allow the study of LepR-dependant interactions in mice (Supplementary Table 1). In order to accomplish this in a micro-PET imaging experiment in mice, with an injected dose of 5-10 MBq, a leptin derivative with a specific activity of at least 500-1000 GBq/μmol would need to be achieved. This extraordinarily high specific activity is not attainable with current radiochemical techniques for protein labeling. Thus, we relied on ex-vivo biodistribution analysis to study Lep-R dependant interactions in mice. In these experiments, a much smaller relative dose of leptin was injected (10-15 KBq corresponding to 0.003 mg/kg vs. 1 mg/kg in PET studies, Supplementary Table 1). Similarly, PET-CT analysis in rhesus macaques requires a much smaller injected dose of tracer in comparison with the size of the animal (0.005 mg/kg, Supplementary Table 1).

The very low brain uptake and biodistribution results are largely consistent with previous leptin biodistribution studies (Banks et al., 1996; Karonen et al., 1998; McMurtry et al., 2004; Van Heek et al., 1996). This profile is not surprising given the small number of leptin binding sites predicted for the hypothalamus. It is remarkable that, despite the fact that many of leptin's biologic outputs are mediated by hypothalamic leptin receptors, such a small fraction of the total hormone produced concentrates in this region (Fig 5c).

We also did not detect hypothalamic binding of leptin in PET studies in monkeys despite the fact that were able to observe saturable binding of leptin to bone marrow. This was likely the result of the extraordinarily high signal in sphenoid bone, which obfuscated any possible signal from the adjacent hypothalamus. Similar studies of leptin binding to hypothalamus in human are less likely to be confounded by this because the human sphenoid is known to pneumatize into an air sinus during development, with low uptake of the proliferation/bone marrow directed tracer ^{18}F-fluorodeoxythymidine (FLT) in this region in adults (Aoki et al., 1989; Buck et al., 2008). Thus these studies provide a basis for of PET studies of leptin biodistribution in humans. If direct binding of leptin in brain can be demonstrated in human, further studies could also provide evidence concerning whether there are differences in the rate of leptin uptake in brain between lean and obese individuals, a possibility that has been previously suggested (Caro et al., 1996).

In summary, here we report the use of two labeled tracers, ^{18}F-FBA-leptin and ^{68}Ga-DOTA-leptin, for PET imaging in rodents and primates. Our two tracers generate identical results, validating the authentic biodistribution of the hormone leptin following systemic administration. Micro-PET imaging in mice revealed that the uptake of leptin by the kidney requires the action of the multiligand endocytic receptor megalin. Additionally, biodistribution analysis and PET imaging in rhesus macaques and mice revealed a high level of uptake of leptin in tissues undergoing active hematopoiesis. The application of our tracers to PET imaging in other systems, including in humans, could provide further information about leptin physiology.

Experimental Procedures

Synthesis of ^{68}Ga-DOTA-leptin and ^{18}F-FBA-Leptin

A lysine-directed labeling approach using DOTA-NHS ester (Macrocyclics) was employed. Briefly, to 100 μL mouse leptin solution at 13.1 mg/mL (Amylin Pharmaceuticals) was added 162 μL metal free (by chelex resin treatment, Biorad) 100 mM sodium phosphate pH 7.5 (final concentration of 5 mg/mL). To this solution was added 100 equivalents of DOTA-NHS (8.2 μmol, 4.1 mg), and the pH adjusted to 7.5 using 1N NaOH. The reaction proceeded for 3 h at 4 °C at which point it was purified by HPLC using a Hewlett Packard 1100 series instrument and a Vydac C4 column (5 micron, 4×150 mm) on a 45-60%B gradient (where buffer A is 0.1% trifluoroacetic acid in water, and buffer B is 90% acetonitrile, 0.1% trifluoroacetic acid in water.) The product was characterized by ESI-MS on a Sciex API-100 single quadrapole spectrometer, which indicated the incorporation of 2-6 DOTA moieties per leptin molecule. The solution was separated to 8 aliquots of DOTA-leptin and lyophilized. Prior to synthesis, the leptin was resuspended in 40 μL of metal free 15 mM HCl, and 10 μL of 1.2M sodium acetate (pH 4.5) was added.

DOTA-Leptin was labeled using ^{68}Ga eluted from a [68]Ge generator (Isotope Products Laboratories) using a previously described procedure (Hoffend et al., 2005) with modifications. We found that reproducible labeling results were obtained by eluting the generator the day prior to labeling, presumably to remove impurities. The gallium generator was eluted with 7 mL of 1M metal free HCl. The solution was diluted with 7 mL of concentrated HCl (trace metal grade, Fisher), and applied to 150 μL settled volume of AG1-X8 resin (Biorad). The ^{68}Ga was then eluted from the resin using 300 μL 15 mM HCl and followed by 100 μL of 15 mM HCl. The dilute acid solution was evaporated at 160 degrees, and the ^{68}Ga was subsequently resuspended in 40 μL of metal free 15 mM HCl. The ^{68}Ga solution was then added to the leptin-DOTA solution (above), and incubated in a 35 °C water bath for 20 minutes. The solution was then centrifuged for 1 min at $10,000 \times g$, and the supernatant added to 2 μL of 0.1M diethylenetriaminepentaacetic acid (DTPA). After 2 min the solution was transferred to a micro bio-spin column 6 (Bio-Rad), which had been pre-equilibrated with PBS according to the manufacturer's instructions. The [68]Ga -DOTA-Leptin was eluted from the column by centrifuging at $1000 \times g$ for 4 minutes. Following elution the solution was diluted to an appropriate volume for injection in PBS (1 mL for rhesus monkey experiments, and 700 uL for two injections in mice), and filtered through a 0.22 μm filter. The specific activity of the conjugate at the end of synthesis was 9.1 ± 4.2 GBq/μmol (s.d., n = 30 syntheses) at greater than 90% pure as determined by radiochemical HPLC and iTLC. The amount of total protein in the reaction was determined by BCA assay (Pierce). ^{18}F-FBA-Leptin was prepared as previously described (Supplemental Fig. 1) (Flavell et al., 2008).

Luciferase reporter assay of Lep-Rb activation

Luciferase reporter assay of Lep-Rb activation was performed as previously described (Flavell et al., 2008). Briefly, bioactivity of mouse recombinant leptin (Amylin Pharmaceuticals) and

semi synthetic derivatives were tested in duplicate for every dilution using a 293 cell line stably transfected with Lep-Rb and a firefly luciferase gene under a STAT3 responsive element. After 24h cells were collected and luciferase activity measured in cell lysate using a luciferase assay system (Promega).

Cell binding experiment

6 aliquots of 20 million Lep-Rb-STAT3-luciferase 293 cells (Flavell et al., 2008) were resuspended in 300 μL HBSS. Approximately $1.4 * 10^5$ CPM of ^{68}Ga-DOTA leptin was added to each tube, with or without cold leptin (Amylin Pharmaceuticals), at a final concentration of 1 μM. The cells were incubated for 2 h, centrifuged, and washed three times with HBSS. The radioactivity associated with the cell pellets, assayed in triplicate, was then counted in a gamma counter.

Mouse studies

Megalin$^{lox/lox}$, ApoE^{cre} and megalin$^{lox/lox}$ mice were obtained from Dr. T. Willnow (Max-Delbrueck Center for Molecular Medicine, Berlin (Leheste et al., 2003). Urine samples for ELISA were collected at 16 weeks of age. Male mice were imaged at seven months of age. Rats used for PET scans were male Sprague-Dawley purchased from Charles Rivers and imaged between 12 and 16 weeks of age. Ob/ob mice used for leptin bioactivity assay were purchased from Jackson Laboratory, and tested at 16 weeks of age when mice were treated with continuous subcutaneous infusion of mouse recombinant leptin or DOTA-leptin using mini osmotic pumps (Alzet) at the dose of 450 ng/h for 10 days.

Ob/ob-Lep-RΔ mice were generated in our laboratory crossing heterozygote mice for both the leptin receptor null mutation (Lep-RΔ) and leptin gene mutation (ob). Ob/ob-Lep-RΔ and ob/ob male mice (genotype was performed by Transnetyx) used for PET scans were imaged between 12 and 16 weeks of age. All mouse studies were conducted under approved protocols of The Rockefeller University and Weill Cornell Medical College.

Micro-PET imaging experiments in mice and rats

In a typical micro-PET mouse experiment, 4-9 MBq of ^{18}F FBA-leptin or ^{68}Ga -DOTA-leptin tracer, corresponding to approximately 25 μg of leptin, was injected in bolus via the tail vein. For rat imaging, 15-30 MBq was injected via the tail vein. Male mice and rats were scanned for 1 hour, under anesthesia with ketamine-xylazine, with continuous bed motion immediately after injection using a micro-PET camera (TM 220, CTI Concord Microsystems, LLC) with a bore size of 22 cm and an axial field of view of 7.6 cm. The resolution at the center of field of view (FOV) is <1.3 mm. 3D histograms of emission data were generated (span3, rig difference 47) using dead time correction. Images were reconstructed using an OSEM2D algorithm without any attenuation or scatter correction. Regions of interest were drawn and images and time activity curves were generated using PMOD biomedical image quantification software.

Biodistribution experiments in mice

Approximately 10-15 KBq of ^{125}I-leptin (New England Nuclear, 81.4 GBq/umol, 20 uL of the solution provided by the manufacturer) was diluted in 300 uL of sterile PBS and injected in the tail vein of the appropriate mouse strains, previously anesthetized with ketamine-xylazine, in the presence of 50 uL of murine leptin solution (13.1 mg/mL, Amylin Pharmaceuticals) or PBS. After 15 minutes, the animals were sacrificed, and tissues were collected and weighed. Radioactivity associated with each sample was counted in a gamma counter with corresponding standards and blanks, and residual activity from each injection. The total injected dose was computed by preparing a standard of 20 uL of the manufacturers' solution, and subtracting the

residual dose remaining in the syringe post injection, and the radioactivity in the tail of the animal.

Primate PET/CT experiments

Subjects were three gonadally intact adult male rhesus monkeys (Macaca mulatta). Subjects were approximately 10-14 years of age and weighed in the range 8-12 kg. Subjects were housed in a stable colony, and were previously exposed to the experimental situation (e.g., pole and collar training, transfer into transport cage etc.). On experiment days, the subjects were individually transported to the PET center in a purpose - built transfer cage. They were then injected with ketamine (10 mg/kg, i.m.) and atropine (0.05 mg/kg, i.m). Subjects were then intubated and anesthesia was induced with isoflurane (3%). Subjects' vital signs (respiratory rate, heart rate, temperature and pulse oximetry) were monitored throughout; anesthesia was typically then maintained at 1.5-2.5% isoflurane for the remainder of the experiment. The subject was placed supine on a heating pad (37°C) in the bed of the PET scanner for the remainder of the experiment. Primate PET/CT scans were performed using a GE Discovery LS PET/CT scanner (GE Healthcare, Waukesha, Wis.). A low-dose CT scan was obtained and the scanner bed was moved into PET position. Competing cold leptin (0.1 mg/kg; i.v. bolus) was administered by a femoral i.v. catheter 5min prior to injection of the radiotracer. Starting 10 min following an intravenous injection of 15 MBq of ^{68}Ga-DOTA-leptin or ^{18}F-FBA-leptin, 4 sequential 20-min whole-body images were obtained (4 beds, 5 minutes each) in 3D acquisition mode. Images were reconstructed using the FORE-Iterative reconstruction method. Following completion of the transmission scan, isoflurane was discontinued, and the subject was extubated when gagging reflex was observed. The subject was carefully observed until recovery (which was rapid and uneventful, in all cases).

All experiments were conducted under approved protocols of the Rockefeller University and Weill Cornell Medical College.

Leptin ELISA, western blotting, HPLC analysis of ^{68}Ga-DOTA-leptin in vitro and in vivo, expression and purification of rhesus leptin and ^{125}I-leptin degradation assay were performed as described in the supplemental methods.

Supplementary Material

Refer to Web version on PubMed Central for supplementary material.

Acknowledgments

References

Aoki S, Dillon WP, Barkovich AJ, Norman D. Marrow conversion before pneumatization of the sphenoid sinus: assessment with MR imaging. Radiology 1989;172:373–375. [PubMed: 2748818]

Bailey, DL.; Townsend, DW.; Valk, PE.; Maisey, MN., editors. Positron Emission Tomography. London: Springer-Verlag; 2005.

Banks WA, Kastin AJ, Huang W, Jaspan JB, Maness LM. Leptin enters the brain by a saturable system independent of insulin. Peptides 1996;17:305–311. [PubMed: 8801538]

Bennett BD, Solar GP, Yuan JQ, Mathias J, Thomas GR, Matthews W. A role for leptin and its cognate receptor in hematopoiesis. Curr Biol 1996;6:1170–1180. [PubMed: 8805376]

Blebea JS, Houseni M, Torigian DA, Fan C, Mavi A, Zhuge Y, Iwanaga T, Mishra S, Udupa J, Zhuang J, et al. Structural and functional imaging of normal bone marrow and evaluation of its age-related changes. Semin Nucl Med 2007;37:185–194. [PubMed: 17418151]

Buck AK, Bommer M, Juweid ME, Glatting G, Stilgenbauer S, Mottaghy FM, Schulz M, Kull T, Bunjes D, Moller P, et al. First Demonstration of Leukemia Imaging with the Proliferation Marker 18F-Fluorodeoxythymidine. J Nucl Med 2008;49:1756–1762. [PubMed: 18927328]

Caro JF, Kolaczynski JW, Nyce MR, Ohannesian JP, Opentanova I, Goldman WH, Lynn RB, Zhang PL, Sinha MK, Considine RV. Decreased cerebrospinal-fluid/serum leptin ratio in obesity: a possible mechanism for leptin resistance. Lancet 1996;348:159–161. [PubMed: 8684156]

Christensen EI, Birn H. Megalin and cubilin: multifunctional endocytic receptors. Nat Rev Mol Cell Biol 2002;3:256–266. [PubMed: 11994745]

Cioffi JA, Shafer AW, Zupancic TJ, Smith-Gbur J, Mikhail A, Platika D, Snodgrass HR. Novel B219/OB receptor isoforms: possible role of leptin in hematopoiesis and reproduction. Nat Med 1996;2:585–589. [PubMed: 8616721]

Claycombe K, King LE, Fraker PJ. A role for leptin in sustaining lymphopoiesis and myelopoiesis. Proc Natl Acad Sci U S A 2008;105:2017–2021. [PubMed: 18250302]

Cohen P, Zhao C, Cai X, Montez JM, Rohani SC, Feinstein P, Mombaerts P, Friedman JM. Selective deletion of leptin receptor in neurons leads to obesity. J Clin Invest 2001;108:1113–1121. [PubMed: 11602618]

Coll AP, Farooqi IS, O'Rahilly S. The hormonal control of food intake. Cell 2007;129:251–262. [PubMed: 17448988]

Cumin F, Baum HP, Levens N. Leptin is cleared from the circulation primarily by the kidney. Int J Obes Relat Metab Disord 1996;20:1120–1126. [PubMed: 8968858]

de Jong M, Barone R, Krenning E, Bernard B, Melis M, Visser T, Gekle M, Willnow TE, Walrand S, Jamar F, et al. Megalin is essential for renal proximal tubule reabsorption of (111)In-DTPA-octreotide. J Nucl Med 2005;46:1696–1700. [PubMed: 16204720]

De Leon-Rodriguez LM, Kovacs Z. The synthesis and chelation chemistry of DOTA-peptide conjugates. Bioconjug Chem 2008;19:391–402. [PubMed: 18072717]

de Luca C, Kowalski TJ, Zhang Y, Elmquist JK, Lee C, Kilimann MW, Ludwig T, Liu SM, Chua SC Jr. Complete rescue of obesity, diabetes, and infertility in db/db mice by neuron-specific LEPR-B transgenes. J Clin Invest 2005;115:3484–3493. [PubMed: 16284652]

Dietrich MO, Spuch C, Antequera D, Rodal I, de Yebenes JG, Molina JA, Bermejo F, Carro E. Megalin mediates the transport of leptin across the blood-CSF barrier. Neurobiol Aging 2008;29:902–912. [PubMed: 17324488]

Farooqi IS, Matarese G, Lord GM, Keogh JM, Lawrence E, Agwu C, Sanna V, Jebb SA, Perna F, Fontana S, et al. Beneficial effects of leptin on obesity, T cell hyporesponsiveness, and neuroendocrine/metabolic dysfunction of human congenital leptin deficiency. J Clin Invest 2002;110:1093–1103. [PubMed: 12393845]

Fei H, Okano HJ, Li C, Lee GH, Zhao C, Darnell R, Friedman JM. Anatomic localization of alternatively spliced leptin receptors (Ob-R) in mouse brain and other tissues. Proc Natl Acad Sci U S A 1997;94:7001–7005. [PubMed: 9192681]

Flavell RR, Kothari P, Bar-Dagan M, Synan M, Vallabhajosula S, Friedman JM, Muir TW, Ceccarini G. Site-specific (18)F-labeling of the protein hormone leptin using a general two-step ligation procedure. J Am Chem Soc 2008;130:9106–9112. [PubMed: 18570424]

Friedman JM, Halaas JL. Leptin and the regulation of body weight in mammals. Nature 1998;395:763–770. [PubMed: 9796811]

Gainsford T, Willson TA, Metcalf D, Handman E, McFarlane C, Ng A, Nicola NA, Alexander WS, Hilton DJ. Leptin can induce proliferation, differentiation, and functional activation of hemopoietic cells. Proc Natl Acad Sci U S A 1996;93:14564–14568. [PubMed: 8962092]

Galloway JL, Zon LI. Ontogeny of hematopoiesis: examining the emergence of hematopoietic cells in the vertebrate embryo. Curr Top Dev Biol 2003;53:139–158. [PubMed: 12510667]

Hama H, Saito A, Takeda T, Tanuma A, Xie Y, Sato K, Kazama JJ, Gejyo F. Evidence indicating that renal tubular metabolism of leptin is mediated by megalin but not by the leptin receptors. Endocrinology 2004;145:3935–3940. [PubMed: 15131016]

Hileman SM, Tornoe J, Flier JS, Bjorbaek C. Transcellular transport of leptin by the short leptin receptor isoform ObRa in Madin-Darby Canine Kidney cells. Endocrinology 2000;141:1955–1961. [PubMed: 10830277]

Karonen SL, Koistinen HA, Nikkinen P, Koivisto VA. Is brain uptake of leptin in vivo saturable and reduced by fasting? Eur J Nucl Med 1998;25:607–612. [PubMed: 9618575]

Klein S, Coppack SW, Mohamed-Ali V, Landt M. Adipose tissue leptin production and plasma leptin kinetics in humans. Diabetes 1996;45:984–987. [PubMed: 8666153]

Leheste JR, Melsen F, Wellner M, Jansen P, Schlichting U, Renner-Muller I, Andreassen TT, Wolf E, Bachmann S, Nykjaer A, et al. Hypocalcemia and osteopathy in mice with kidney-specific megalin gene defect. FASEB J 2003;17:247–249. [PubMed: 12475886]

Lord GM, Matarese G, Howard JK, Baker RJ, Bloom SR, Lechler RI. Leptin modulates the T-cell immune response and reverses starvation-induced immunosuppression. Nature 1998;394:897–901. [PubMed: 9732873]

McCarthy TJ, Banks WA, Farrell CL, Adamu S, Derdeyn CP, Snyder AZ, Laforest R, Litzinger DC, Martin D, LeBel CP, et al. Positron emission tomography shows that intrathecal leptin reaches the hypothalamus in baboons. J Pharmacol Exp Ther 2002;301:878–883. [PubMed: 12023514]

McMurtry JP, Ashwell CM, Brocht DM, Caperna TJ. Plasma clearance and tissue distribution of radiolabeled leptin in the chicken. Comp Biochem Physiol A Mol Integr Physiol 2004;138:27–32. [PubMed: 15165567]

Merabet E, Dagogo-Jack S, Coyne DW, Klein S, Santiago JV, Hmiel SP, Landt M. Increased plasma leptin concentration in end-stage renal disease. J Clin Endocrinol Metab 1997;82:847–850. [PubMed: 9062494]

Meyer C, Robson D, Rackovsky N, Nadkarni V, Gerich J. Role of the kidney in human leptin metabolism. Am J Physiol 1997;273:E903–907. [PubMed: 9374675]

Morioka T, Asilmaz E, Hu J, Dishinger JF, Kurpad AJ, Elias CF, Li H, Elmquist JK, Kennedy RT, Kulkarni RN. Disruption of leptin receptor expression in the pancreas directly affects beta cell growth and function in mice. J Clin Invest 2007;117:2860–2868. [PubMed: 17909627]

Palmer G, Aurrand-Lions M, Contassot E, Talabot-Ayer D, Ducrest-Gay D, Vesin C, Chobaz-Peclat V, Busso N, Gabay C. Indirect effects of leptin receptor deficiency on lymphocyte populations and immune response in db/db mice. J Immunol 2006;177:2899–2907. [PubMed: 16920925]

Peelman F, Van Beneden K, Zabeau L, Iserentant H, Ulrichts P, Defeau D, Verhee A, Catteeuw D, Elewaut D, Tavernier J. Mapping of the leptin binding sites and design of a leptin antagonist. J Biol Chem 2004;279:41038–41046. [PubMed: 15213225]

Raila J, Willnow TE, Schweigert FJ. Megalin-mediated reuptake of retinol in the kidneys of mice is essential for vitamin A homeostasis. J Nutr 2005;135:2512–2516. [PubMed: 16251603]

Schottelius M, Poethko T, Herz M, Reubi JC, Kessler H, Schwaiger M, Wester HJ. First (18)F-labeled tracer suitable for routine clinical imaging of sst receptor-expressing tumors using positron emission tomography. Clin Cancer Res 2004;10:3593–3606. [PubMed: 15173065]

Sierra-Honigmann MR, Nath AK, Murakami C, Garcia-Cardena G, Papapetropoulos A, Sessa WC, Madge LA, Schechner JS, Schwabb MB, Polverini PJ, et al. Biological action of leptin as an angiogenic factor. Science 1998;281:1683–1686. [PubMed: 9733517]

Thomas T, Gori F, Khosla S, Jensen MD, Burguera B, Riggs BL. Leptin acts on human marrow stromal cells to enhance differentiation to osteoblasts and to inhibit differentiation to adipocytes. Endocrinology 1999;140:1630–1638. [PubMed: 10098497]

Tsai SW, Li L, Williams LE, Anderson AL, Raubitschek AA, Shively JE. Metabolism and renal clearance of 111In-labeled DOTA-conjugated antibody fragments. Bioconjug Chem 2001;12:264–270. [PubMed: 11312688]

Umemoto Y, Tsuji K, Yang FC, Ebihara Y, Kaneko A, Furukawa S, Nakahata T. Leptin stimulates the proliferation of murine myelocytic and primitive hematopoietic progenitor cells. Blood 1997;90:3438–3443. [PubMed: 9345027]

Van Heek M, Mullins DE, Wirth MA, Graziano MP, Fawzi AB, Compton DS, France CF, Hoos LM, Casale RL, Sybertz EJ, et al. The relationship of tissue localization, distribution and turnover to feeding after intraperitoneal 125I-leptin administration to ob/ob and db/db mice. Horm Metab Res 1996;28:653–658. [PubMed: 9013736]

Verploegen SA, Plaetinck G, Devos R, Van der Heyden J, Guisez Y. A human leptin mutant induces weight gain in normal mice. FEBS Lett 1997;405:237–240. [PubMed: 9089297]

Vila R, Adan C, Rafecas I, Fernandez-Lopez JA, Remesar X, Alemany M. Plasma leptin turnover rates in lean and obese Zucker rats. Endocrinology 1998;139:4466–4469. [PubMed: 9794453]

Zeng J, Patterson BW, Klein S, Martin DR, Dagogo-Jack S, Kohrt WM, Miller SB, Landt M. Whole body leptin kinetics and renal metabolism in vivo. Am J Physiol 1997;273:E1102–1106. [PubMed: 9435524]

Zhang F, Basinski MB, Beals JM, Briggs SL, Churgay LM, Clawson DK, DiMarchi RD, Furman TC, Hale JE, Hsiung HM, et al. Crystal structure of the obese protein leptin-E100. Nature 1997;387:206–209. [PubMed: 9144295]

Zlokovic BV, Martel CL, Matsubara E, McComb JG, Zheng G, McCluskey RT, Frangione B, Ghiso J. Glycoprotein 330/megalin: probable role in receptor-mediated transport of apolipoprotein J alone and in a complex with Alzheimer disease amyloid beta at the blood-brain and blood-cerebrospinal fluid barriers. Proc Natl Acad Sci U S A 1996;93:4229–4234. [PubMed: 8633046]
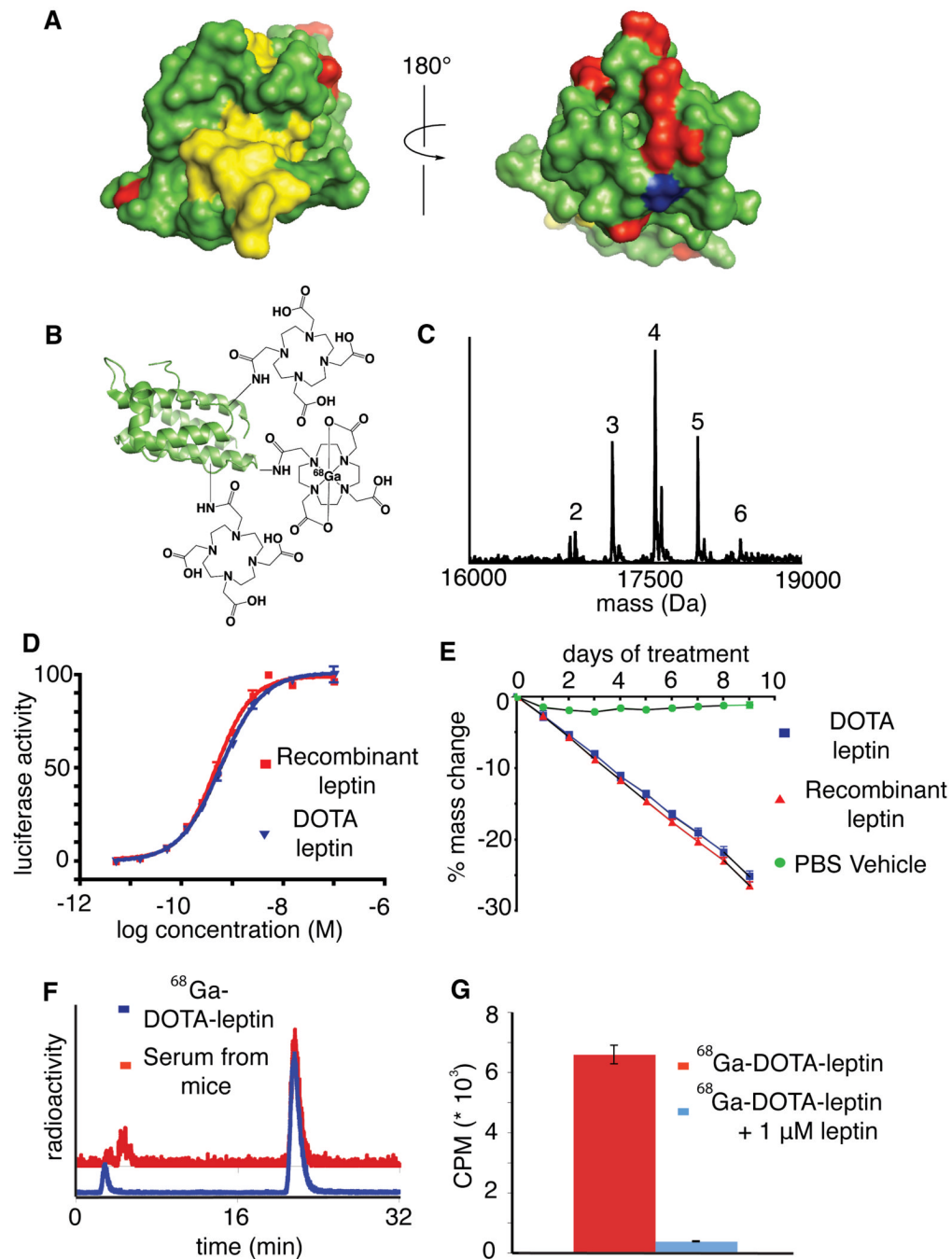
Figure 1. Design, synthesis, and biological activity of the tracer ^{68}Ga-DOTA-leptin
A) Two surface rendered-views of the structure of leptin (PDB ID 1AX8). Residues which are essential for Lep-R activation are rendered in yellow, while the amines (the sites of labeling in ^{68}Ga-DOTA-leptin) are rendered in red and the C-terminus (the site of labeling in ^{18}F-FBA-leptin) is rendered in blue. B) Schematic of ^{68}Ga-DOTA-leptin tracer. C) ESI-MS of DOTA-leptin revealing an average of 4 copies of DOTA per leptin molecule. D) *in vitro* bioactivity of DOTA-leptin was compared to recombinant leptin using a cell line stably expressing leptin receptor (Lep-Rb) and a luciferase reporter under STAT3 responsive element. The EC_{50} for activation was 0.42 to 0.55 nM for recombinant leptin and 0.54 to 0.66 nM for DOTA-leptin (95% confidence intervals). E) DOTA-leptin induces weight loss to a similar extent as

recombinant leptin in ob/ob mice (n=4, dose = 450 ng/hr). F) Radiochemical RP-HPLC analysis of purified ^{68}Ga-DOTA-leptin (blue) and serum recovered from a mouse 30 min post injection with ^{68}Ga-DOTA-leptin. G) Cell binding assay of ^{68}Ga-DOTA-leptin using a 293 cell line expressing Lep-Rb, in the presence or absence of 1 μM competing recombinant leptin (n=3, mean ± SEM).
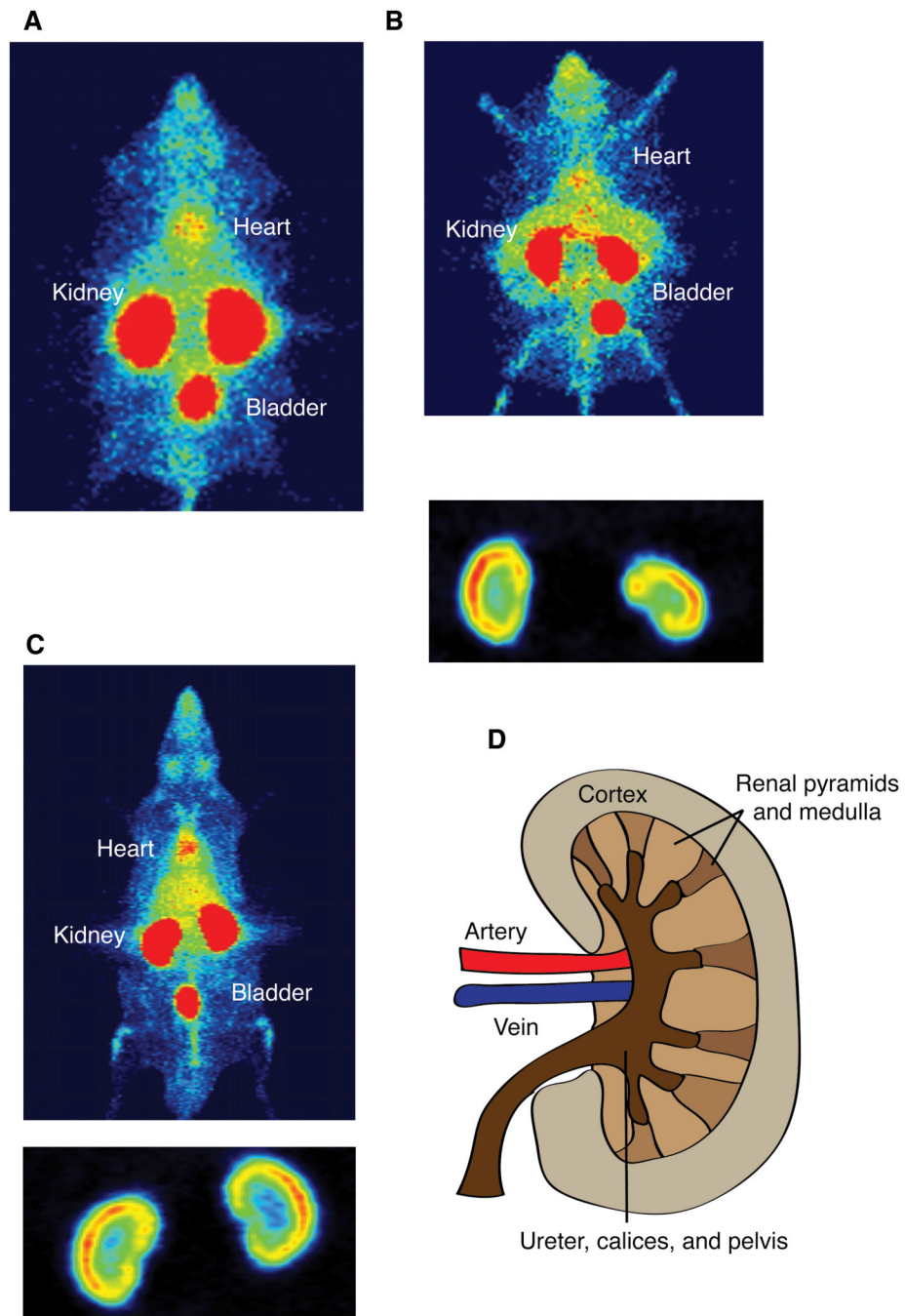
Figure 2. Whole body PET images of mice and rats reveal that leptin is taken up in the cortex of the kidney

The images are overexposed to reveal areas with a lower level of uptake. A) Whole body PET maximum intensity projection (MIP) image of a leptin deficient (ob/ob) mouse injected with ^{68}Ga-DOTA-leptin. Renal uptake of leptin in ob/ob mice is 65.1% ± 3.5% while the bladder is only 2.2 ± 0.2% over 30 min. Uptake in other organs is lower than this per volume. B) Whole body PET coronal MIP image of an ob/ob mouse injected with ^{18}F-FBA-leptin, with inset of kidneys with lowered contrast, revealing uptake of the hormone in the renal cortex. C) Whole body PET coronal MIP of a Sprague-Dawley rat injected with ^{68}Ga-DOTA-leptin, with

inset with lowered contrast, revealing uptake of the hormone in the cortex of the kidney. D) Simplified diagram of renal anatomy.

A

B

C

D
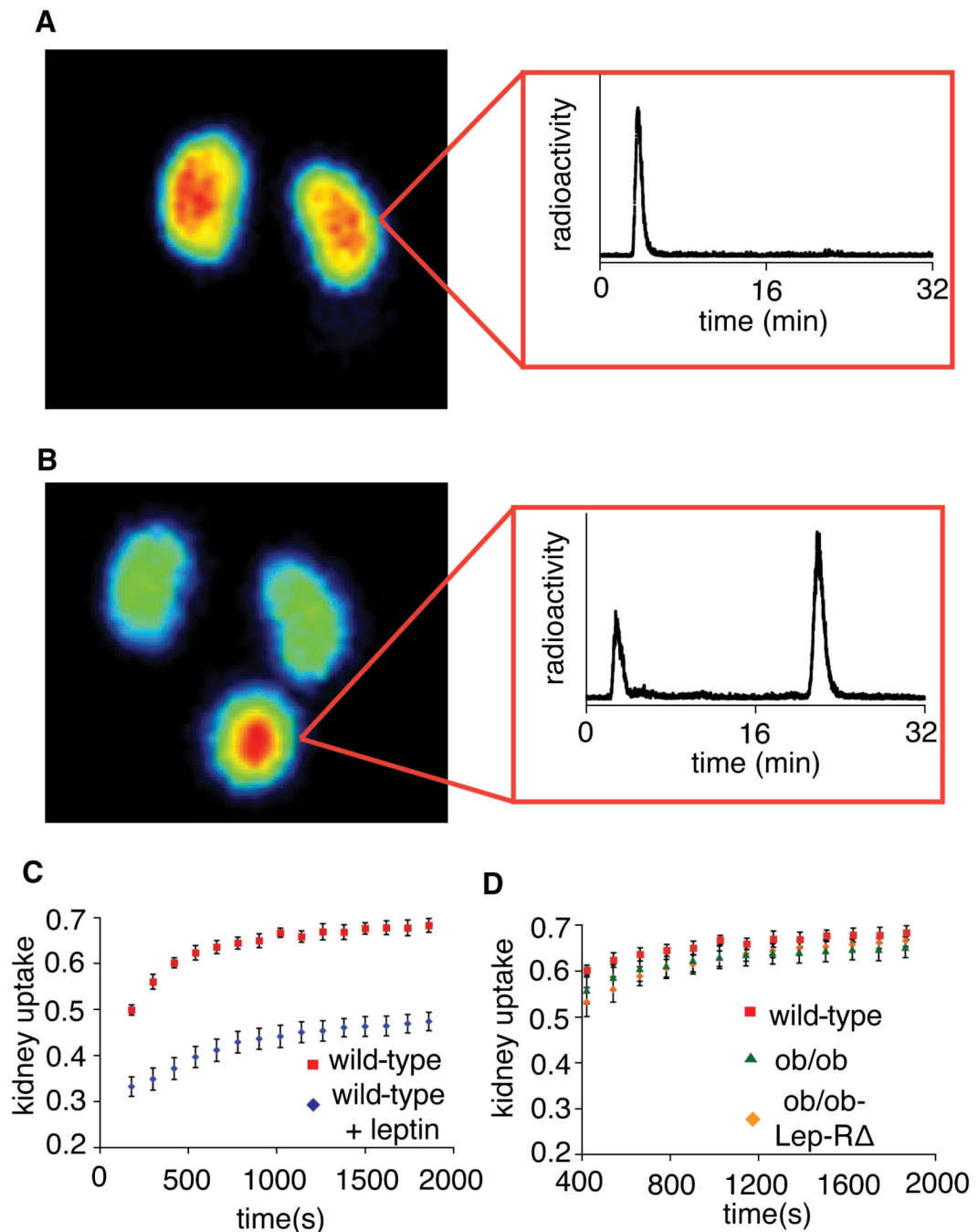
Figure 3. Blocking experiments of leptin uptake in the kidney inwild type mice, and analysis of uptake in Lep-R deficient animals

A) Coronal maximum intensity projection (MIP) of a C57Bl6 wild type mouse injected with ^{68}Ga-DOTA-leptin, with inset of radiochemical RP-HPLC analysis of homogenized kidneys one hour post injection with ^{68}Ga-DOTA-leptin. B) Coronal MIP of a C57Bl6 wild type mouse co-injected with ^{68}Ga-DOTA-leptin and 650 μg leptin, with inset of a radiochemical RP-HPLC analysis of the urine 30 minutes post injection. C) Time activity curves of the kidney of C57Bl6 wild type mice injected with ^{68}Ga-DOTA-leptin in the presence or absence of 650 μg leptin. All data are reported as means (n=3) ± s.e.m. Statistical significance of the difference between the two groups was assessed by Student's t-test, p< 0.01 for all time

points. D) A comparison of the uptake of ^{68}Ga-DOTA-leptin in the kidneys of wild type C57Bl6, ob/ob, and ob/ob-Lep-RΔ mice.
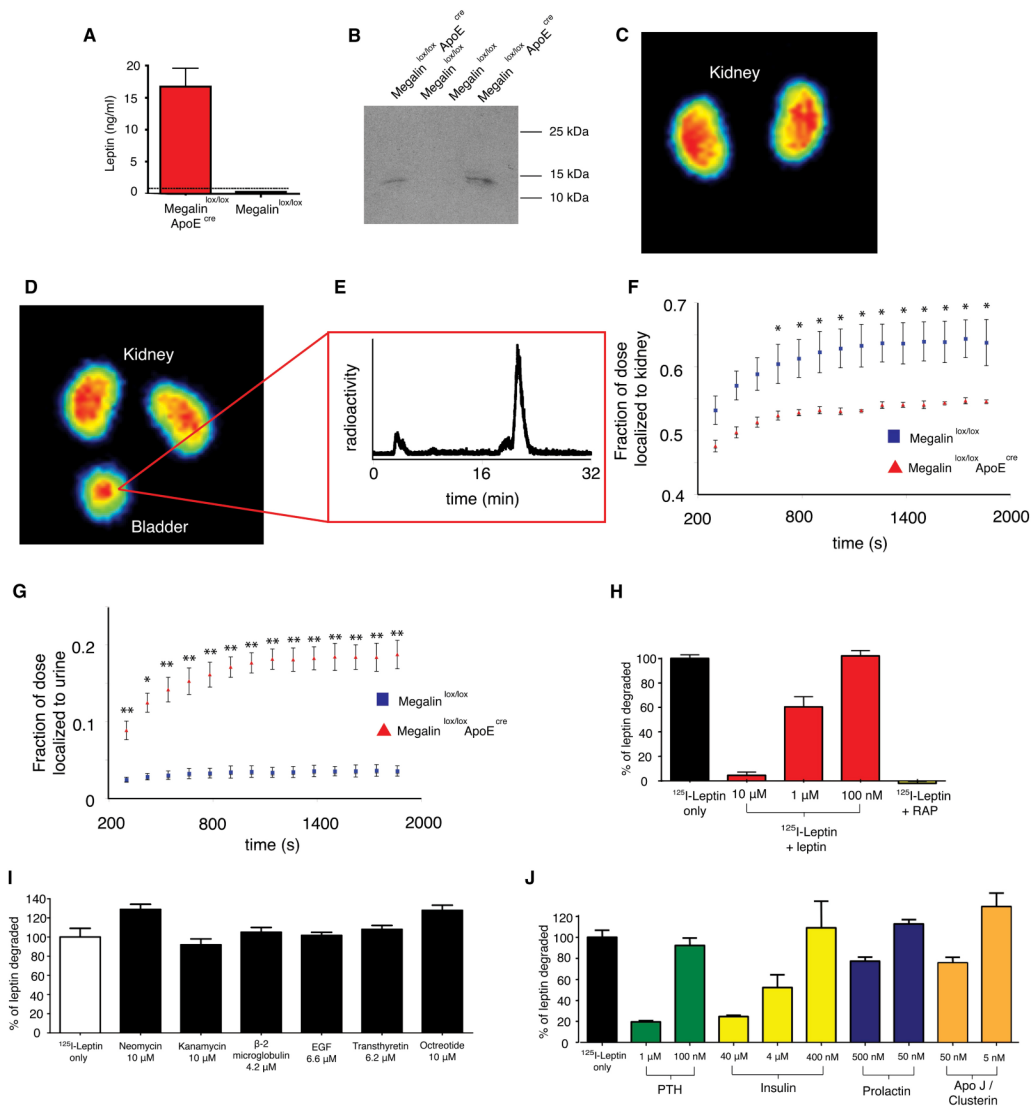
Figure 4. Role of megalin in the *in vivo* uptake of leptin in the kidney and in L2 cells
A) Enzyme-Linked ImmunoSorbent Assay (ELISA) of leptin in the urine of the indicated mouse strains. The dotted line represents the limit of detection of the assay (n=3 ± SEM, statistical significance of difference between Megalin[lox/lox]ApoE[Cre] and Megalin[lox/lox]: p<0.001). B) Anti-leptin western blot of the urine of megalin[lox/lox] ApoE[cre] and megalin[lox/lox] controls. C-D) Coronal MIP of a megalin[lox/lox] control mouse (C) injected with ^{68}Ga-DOTA-leptin and of a megalin[lox/lox] ApoE[cre] mouse (D) injected with ^{68}Ga-DOTA-leptin. E) Radiochemical RP-HPLC analysis of urine recovered from a megalin[lox/lox] ApoE[cre] mouse, which was injected with ^{68}Ga-DOTA-leptin. f, g) Time activity curves of the uptake in the kidney (F) and bladder (G) of ^{68}Ga-DOTA-leptin in megalin[lox/lox] ApoE[cre] and megalin[lox/lox] mice. All data are reported as mean ± SEM (n=3). Statistical significance of megalin kidney KO versus lox controls: * p < 0.05, ** p < 0.01.
H) Leptin is degraded by an L2 yolk sac tumor cell line, and the degradation can be inhibited by competing cold leptin or receptor associated protein (RAP, 100 μg/mL) I-J) Degradation of leptin by L2 cells can be inhibited by some megalin ligands but not others.
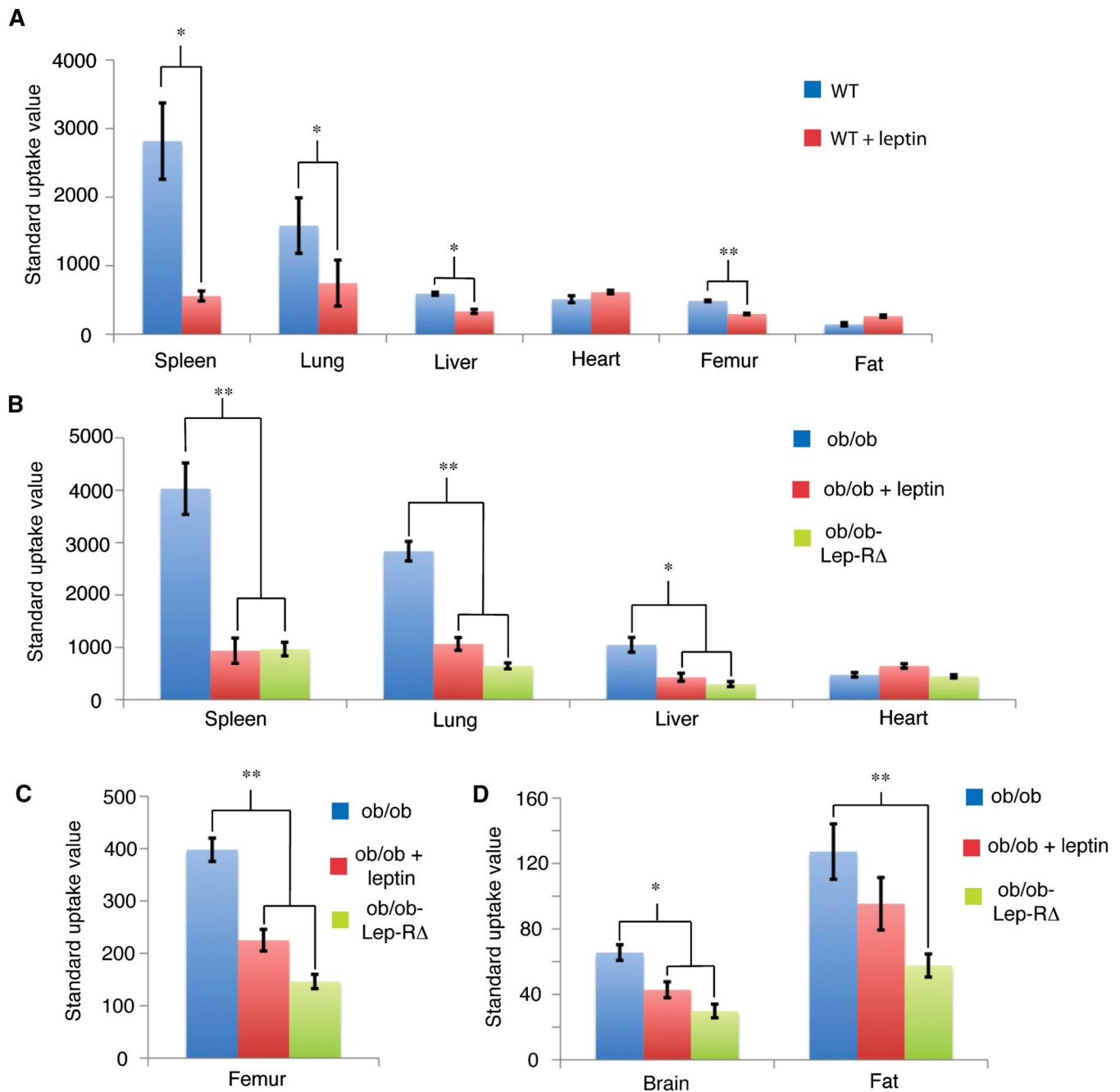
Figure 5. Biodistribution studies of ^{125}I-leptin in mice
From 8-12 KBq of ^{125}I-leptin was injected into the tail vein of the indicated mouse strains. The animals were sacrificed 15 minutes post injection, the indicated tissues removed, weighed and the radioactivity counted. Standard uptake value on the Y-axis is defined as the % injected dose/gram of tissue, divided by % injected dose per mg of blood. This analysis is used to correct for the varying levels of leptin in the blood in the different animal groups (Supplemental Table 2). Results are represented as means ± SEM (n = 3-4 per experimental group). Statistical significance between groups was assessed by Student's t-test (*: p < 0.05, **: p < 0.01). A) Uptake in organs compared between wild type animals and wild type animals with 650 μg

leptin co-injection. B-D) Uptake in organs compared between ob/ob mice, ob/ob mice with 650 μg leptin co-injection, and ob/ob-Lep-RΔ mice.
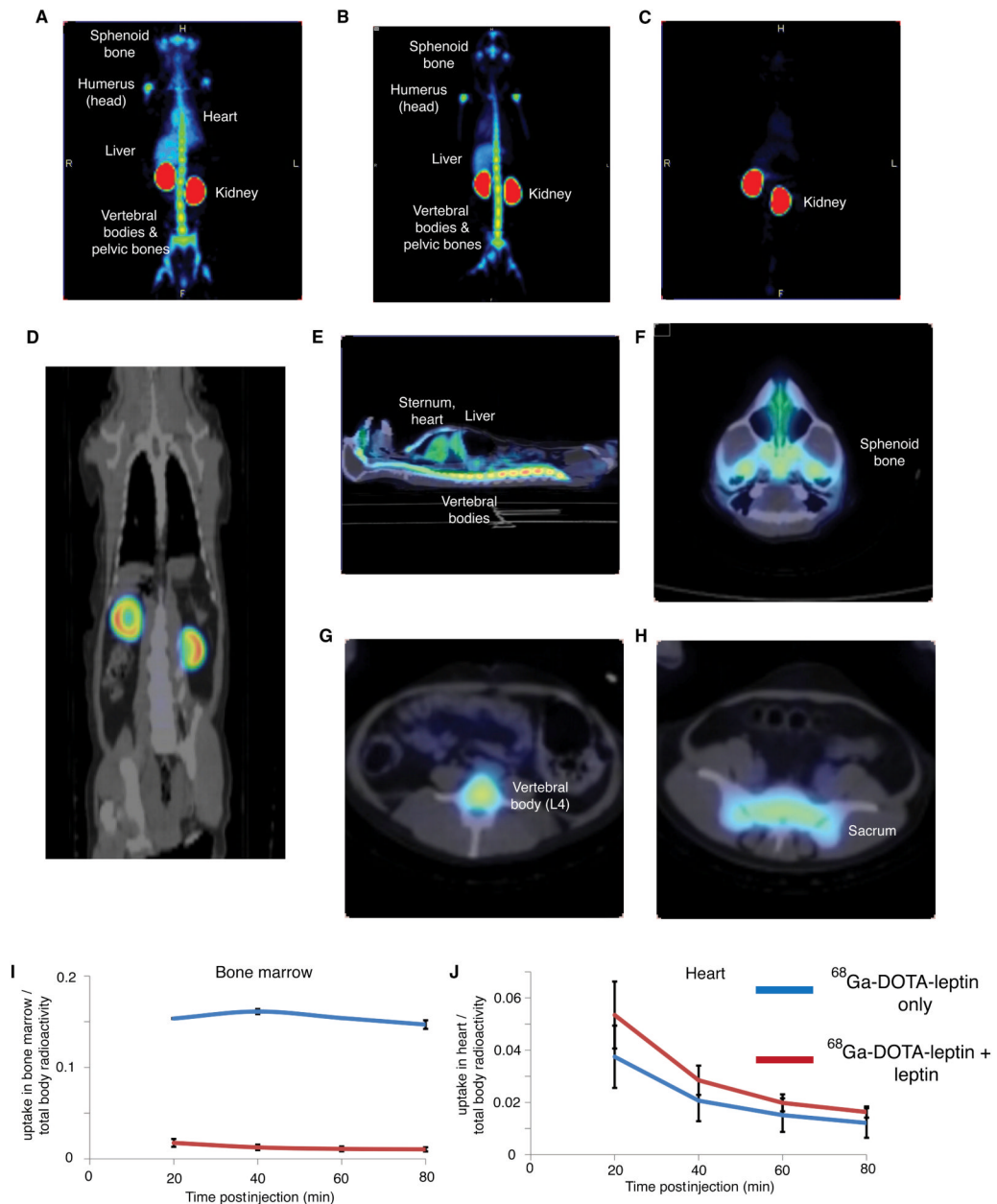
Figure 6. PET imaging study of leptin biodistribution in rhesus macaques
Images were acquired 10 minutes post injection of 15 MBq ^{68}Ga-DOTA-leptin or ^{18}F-FBA-leptin. A-B) Coronal MIP acquired 10 minutes post injection of ^{68}Ga-DOTA-leptin (A) or ^{18}F-FBA-leptin (B). C) Coronal MIP of a rhesus macaque acquired 10 minutes post injection of 15 MBq ^{68}Ga-DOTA-leptin, with pre-treatment with 1 mg of rhesus leptin 5 minutes before radiotracer injection. D) Coronal PET-CT fusion revealing uptake of the tracer in the cortex of the kidney. E) Sagittal PET-CT fusion revealing uptake of the tracer in the vertebral bodies, sternum, liver, and presence of the tracer in the blood pool. F-H) Axial PET-CT sections through the sphenoid bone of the base of the skull (F), the L4 vertebral body (G), and the sacrum (H). I-J) Time activity curves of ^{68}Ga-DOTA-leptin uptake in the bone marrow (I) and heart (J). The y axis on the TACs represents the % of total injected dose localized to that tissue.